Journal of Sound and Vibration (1997) **205**(1), 1–18

SYSTEM IDENTIFICATION FROM AMBIENT VIBRATION MEASUREMENTS ON A BRIDGE

C. R. FARRAR

*MS P*946, *Los Alamos National Laboratory*, *Los Alamos*, *New Mexico* 87545, *U.S.A.*

AND

G. H. JAMES III

Sandia National Laboratories, *Albuquerque*, *New Mexico* 87185, *U.S.A.*

(*Received* 4 *September* 1996, *and in final form* 24 *January* 1997)

The cross-correlation function between two response measurements made on an ambiently excited structure is shown to have the same form as the system's impulse response function. Therefore, standard time domain curve-fitting procedures, which are typically applied to impulse response functions, can now be applied to the cross-correlation functions to estimate the resonant frequencies and modal damping of the structure. This derivation is based on the assumption that the ambient vibration source is a white noise random process. Curve-fitting cross-correlation functions to obtain modal properties offers advantages over standard procedures that identify resonant frequencies from peaks in the power spectrum and damping from the width of the power spectrum. The primary advantage is the ability to identify closely spaced modes and their associated damping. The resonant frequencies of a highway bridge that were identified by curve-fitting the cross-correlation functions, using traffic excitation as the ambient vibration source, are compared to modal properties identified by standard forced vibration testing methods. Results of this comparison showed a maximum discrepancy of 3·63 percent. Similar comparisons for the average modal damping values identified by the two methods showed a 9·82 percent difference. This experimental verification implies that the proposed method of analyzing ambient vibration data can be used to accurately assess the dynamic properties of structures in a non-intrusive manner.

1. INTRODUCTION

For both newly constructed bridges and for older existing bridges, it is desirable to measure the dynamic properties (resonant frequencies, mode shapes and modal damping) of the bridges to understand better their dynamic behavior under normal traffic loads as well as extreme loads such as those caused by seismic events or high winds. These measured properties can be used to update numerical models of the bridge so that these models better reflect the *in situ* boundary conditions and as-built structural connectivity. Also, periodic monitoring of the dynamic properties is being studied for possible use as a method to assess degradation in the structural integrity of the bridge. Under normal operating conditions, knowledge of the dynamic properties can be used to assess the effects of traffic loading on the fatigue life of the structure and to determine dynamic load factors for these structures.

Typically in vibration testing, analytical forms of frequency response functions (FRF) relating a measured input, usually force, to a measured response such as acceleration are fit to measured FRFs to estimate the dynamic properties of a structure. The use of

0022–460X/97/310001 + 18 $25.00/0/sv970977

measured input-measured response FRFs to identify a structure's dynamic properties is well documented in the technical literature [1]. However, when a bridge is subjected to traffic excitation, it is difficult, if not impossible, to measure the input to the structure. The extension of system identification methods to ambient vibration cases, in which an input cannot be measured, has received considerably less attention in the technical literature. However, the size of most bridges and the disruption of traffic flow if they are taken out of service typically makes ambient vibration testing the only practical experimental method available for studying their dynamic response.

One of the earliest attempts fully to characterize the dynamic parameters of bridges undergoing ambient vibrations was reported by McLamore, Hart and Stubbs [2], using an extension of a spectral technique developed by Crawford and Ward [3]. In this work, the recorded motion of the bridge was measured with a series of accelerometers. Frequencies associated with peaks in the power spectral density function (PSD) of each recorded motion provided estimates of resonant frequencies. The half-power bandwidth method (HPBW) was used to estimate the modal damping associated with these peaks. Amplitude and phase information contained in cross-power spectra (CPS) between a designated reference measurement and the other measurements provided estimates of mode shapes. This method of system identification from ambient response measurements has been summarized more recently by Bendat and Piersol [4]. Following this earlier work, numerous ambient vibration tests, most of which analyze the response measurements in a manner similar to that presented by McLamore, Hart and Stubbs, have been reported. These ambient bridge tests are summarized in references [5–23]. Drawbacks of the system identification methods used in these studies, which have been previously identified by Abdel Gaffar and Housner [5], are the need for very high frequency resolution (the necessary resolution has been quantified in reference [4]) around the resonance to adequately define the half-power points and the difficulties in identifying closely spaced modes because of spectral overlap.

Other methods of extracting modal parameters from ambient vibration data have made use of averaged, normalized PSDs to estimate the resonant frequencies. A modal ratio function that weights the frequency response function magnitude and phase information between a designated reference measurement and other measurements with a discrete binary function derived from the coherence function is then used to estimate modal amplitudes and phases [24–27]. This method also suffers from the difficulties associated with closely spaced modes discussed above. Autoregressive moving average models [28], random decrement analysis [29], and time–frequency analysis methods [30] have also been applied to ambient vibration system identification [29], and a direct comparison of these methods is presented in reference [31]. However, these methods require the development of algorithms not typically implemented in most data acquisition and analysis software.

In this paper an ambient vibration system identification method, referred to as the Natural Excitation Technique (NExT) [32, 33], is presented, which circumvents the drawbacks of the methods previously discussed and can be implemented through algorithms found in almost all commercial signal analysis software packages. The NExT method essentially involves applying time domain curve-fitting algorithms to cross-correlation measurements made between various response measurements on an ambiently excited structure to estimate the resonant frequencies and modal damping. To justify such a system identification procedure, it must be shown that for an input, which is not measured but assumed to be white noise, the cross-correlation function between two response measurements is the sum of decaying sinusoids and these decaying sinusoids have the same damped resonant frequencies and damping ratios as the modes of the system. This result implies the cross-correlation functions will have

the same form as the system's impulse resonse function. Therefore, time domain curve-fitting algorithms such as the polyreference method [34], the complex exponential method [35] or the eigensystem realization algorithm [36], which were developed to analyze impulse response functions, can be applied to the cross-correlation functions to obtain the resonant frequencies and modal damping exhibited by the structure.

The polyreference method, the complex exponential curve-fitting method and the eigensystem realization algorithm are classified as multi-degree-of-freedom methods, because they attempt to simultaneously identify all modes within a given frequency range and to compensate for the influence of out-of-band modes. Therefore, these curve-fitting methods account for the spectral overlap that has caused problems for the methods used in previous studies. The proposed method has the ability to identify dynamic properties associated with closely spaced modes. Mode shapes are again determined from magnitudes and phases in the CPS at the identified resonant frequencies. The method is demonstrated by analyzing ambient traffic-induced vibration data from a 130 m (425 ft) section of a highway bridge, and results are compared to dynamic properties identified from conventional forced vibration tests conducted after traffic was removed from the bridge.

2. BASIS OF THE ANALYSIS METHOD

For an n-degree-of-freedom system, the equations of motion can be represented in matrix form as

$$[m]\{\ddot{x}(t)\} + [c]\{\dot{x}(t)\} + [k]\{x(t)\} = \{f(t)\}, \tag{1}$$

where $[m]$ is the $n \times n$ mass matrix, $[c]$ is the $n \times n$ damping matrix, $[k]$ is the $n \times n$ stiffness matrix, $\{\ddot{x}(t)\}$ is the $n \times 1$ acceleration vector, $\{\dot{x}(t)\}$ is the $n \times 1$ velocity vector, $\{x(t)\}$ is the $n \times 1$ displacement vector, and $\{f(t)\}$ is the $n \times 1$ applied force vector.

When proportional damping is assumed and equation (1) is transformed into modal co-ordinates, a set of uncoupled scalar equations of the following form results:

$$\ddot{q}^r + 2\zeta^r\omega_n^r\dot{q}^r + (\omega_n^r)^2 q^r = \frac{1}{m^r}\{\phi^r\}^{\mathrm{T}}\{f(t)\}, \tag{2}$$

where the superscript r denotes values associated with the rth mode, q, $\dot{q}$ and $\ddot{q}$ are the displacement, velocity and acceleration in modal co-ordinates, ϕ is the mode shape vector, ω_n is the natural frequency, and m is the modal mass. These equations may be solved by the convolution integral, assuming a general forcing function and zero initial condition, and back-transformed into the original co-ordinates, yielding

$$\{x\} = \sum_{r=1}^{n}\{\phi^r\}^{\mathrm{T}}\int_{-\infty}^{t}\{\phi^r\}^{\mathrm{T}}\{f(\tau)g^r(t-\tau)\,\mathrm{d}\tau, \tag{3}$$

where $g^r(t) = (1/m^r\omega_d^r)\,\mathrm{e}^{-\zeta^r\omega_n^r t}\sin(\omega_d^r t)$ is the impulse response function associated with mode r, ω_d^r is the damped natural frequency associated with mode r and n is the number of modes.

The response at location i caused by an input at location k, x_{ik} and $f_k(t)$, respectively, can be expressed as

$$x_{ik} = \sum_{r=1}^{n}\phi_i^r\phi_k^r\int_{-\infty}^{t}f_k(\tau)g^r(t-\tau)\,\mathrm{d}\tau, \tag{4}$$

where ϕ_i^r is the ith component of the mode shape vector.

If $f(\tau)$ is a Dirac delta function at $\tau = 0$, then the response at location i resulting from the impulse at location k is

$$x_{ik} = \sum_{r=1}^{n} \frac{\phi_i^r \phi_k^r}{m^r \omega_d^r} e^{-\zeta^r \omega_n^r t} \sin(\omega_d^r t). \tag{5}$$

The cross-correlation function $R_{ijk}(t)$ relating two measured responses at locations i and j caused by a white noise random input at k is given by Bendat and Pierson [4] as

$$R_{ijk}(T) = \mathrm{E}\{x_{ik}(t+T)x_{jk}(t)\}, \tag{6}$$

where $\mathrm{E}\{\}$ indicates the expectation operator.

Substituting equation (4) into equation (6) and noting that $f_k(t)$ is the only random variable yields

$$R_{ijk}(T) = \sum_{r=1}^{n}\sum_{s=1}^{n} \phi_i^r \phi_k^r \phi_j^s \phi_k^s \int_{-\infty}^{t}\int_{-\infty}^{t+T} g^r(t+T-\sigma) g^s(t-\tau) \mathrm{E}\{f_k(\sigma) f_k(\tau)\}\, \mathrm{d}\sigma\, \mathrm{d}\tau. \tag{7}$$

On the basis of the assumption that $f(t)$ is a white noise function, and using the definition of the autocorrelation function given in reference [4], the following relationship can be established for the autocorrelation function of f:

$$\mathrm{E}\{f_k(\sigma) f_k(\tau)\} = \alpha_k \delta(\tau - \sigma), \tag{8}$$

where α_k is a constant and $\delta(t)$ is the Dirac delta function.

Substituting equation (8) into equation (7) and changing the variable of integration to $\lambda = t - \tau$ yields

$$R_{ijk}(T) = \sum_{r=1}^{n}\sum_{s=1}^{n} \alpha_k \phi_i^r \phi_k^r \phi_j^s \phi_k^s \int_0^{\infty} g^r(\lambda + T) g^s(\lambda)\, \mathrm{d}\lambda. \tag{9}$$

From the previous definition of g^r and the trigonometric identity for the sine of a sum, $g^r(\lambda + T)$ can be expressed with terms involving T separated from those involving λ, resulting in

$$g^r(\lambda + T) = [e^{-\zeta^r \omega_n^r T} \cos(\omega_d^r T)] \frac{e^{-\zeta^r \omega_n^r \lambda} \sin(\omega_d^r \lambda)}{m^r \omega_d^r} + [e^{-\zeta^r \omega_n^r T} \sin(\omega_d^r T)] \frac{e^{-\zeta^r \omega_n^r \lambda} \cos(\omega_d^r \lambda)}{m^r \omega_d^r}. \tag{10}$$

When equation (10) is substituted into equation (9) along with the corresponding term for $g^s(\lambda)$, the terms involving T can be factored out of the integral and the summation on s yields the following form for the cross-correlation function:

$$R_{ijk}(T) = \sum_{r=1}^{n} G_{ijk}^r [e^{-\zeta^r \omega_n^r T} \cos(\omega_d^r T)] + H_{ijk}^r [e^{-\zeta^r \omega_n^r T} \sin(\omega_d^r T)], \tag{11}$$

where

$$\begin{Bmatrix} G_{ijk}^r \\ H_{ijk}^r \end{Bmatrix} = \sum_{s=1}^{n} \frac{\alpha_k \phi_i^r \phi_k^r \phi_j^s \phi_k^s}{m^r \omega_d^r m^s \omega_d^s} \int_0^{\infty} e^{(-\zeta^r \omega_n^r - \zeta^s \omega_n^s)\lambda} \sin(\omega_d^r \lambda) \begin{Bmatrix} \sin(\omega_d^r \lambda) \\ \cos(\omega_d^r \lambda) \end{Bmatrix} \mathrm{d}\lambda. \tag{12}$$

From equations (11) and (12), it is evident that the cross-correlation functions between two response measurements that result from an unknown white noise excitation have the form of decaying sinusoids, and these decaying sinusoids have the same characteristics as the system's impulse response function. Therefore time domain system identification techniques, which are typically applied to impulse response functions, can be applied to these cross-correlation functions to estimate the system's resonant frequencies and modal damping values. This derivation is based on those summarized in references [32, 33]. The ambient vibration system identification method is now applied to ambient vibration data from traffic excitation obtained on a highway bridge.

When implemented in practice, the cross-power spectrum is first estimated and then inverse Fourier transformed to obtain the cross-correlation function. Therefore, this method will be subject to window-dependent resolution bias errors as discussed in reference [37]. These errors also influence standard curve-fitting procedures that are applied to measured-input frequency response functions. As with frequency response function estimates, random errors associated with the cross-power spectrum can be minimized by averaging numerous measurement samples [4]. The effects of bias error sources were not investigated in this study. Measurement averaging was employed to minimize the random error sources.

3. TEST STRUCTURE

The former I-40 bridge over the Rio Grande (this structure was replaced in 1993) consisted of twin spans made up of a concrete deck supported by two welded steel plate girders and three steel stringers. Loads from the stringers were transferred to the plate girders by floor beams located at approximately 6·1 m (20 ft) intervals. Cross-bracing was provided between the floor beams. Each span carried three lanes of traffic under normal operating conditions. In Figure 1 is shown an elevation view of the portion of the bridge that was tested. The cross-section geometry of the bridge is shown in Figure 2.

Each bridge was made up of three identical sections. Except for the common pier located at the end of each section, the sections are independent. A section had three spans; the end spans are of equal length, approximately 39·9 m (131 ft), and the center span was approximately 49·7 m (163 ft) long. Five plate girders were connected with four bolted splices to form a continuous beam over the three spans. The portions of the plate girders over the piers had increased flange dimensions, compared with the mid-span portions, to resist the higher bending stresses at these locations. Connections that allowed for

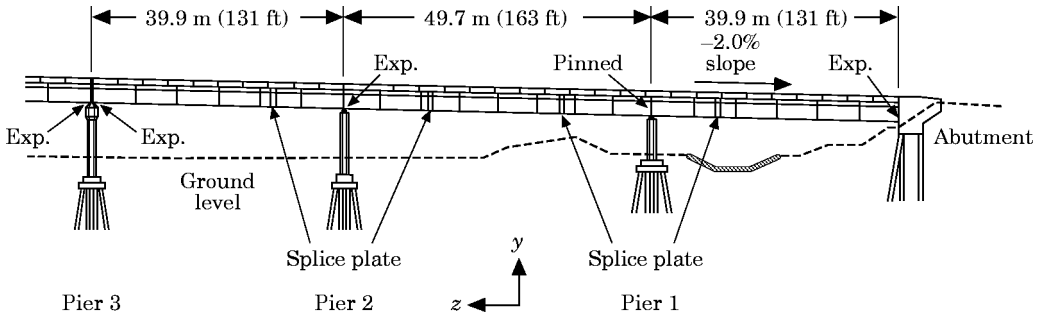

Figure 1. An elevation view of the portion of the eastbound bridge that was tested.

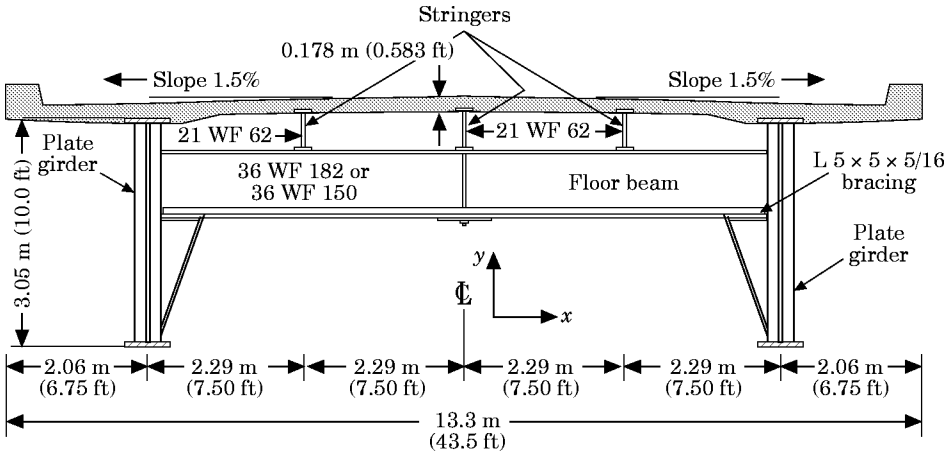

Figure 2. A typical cross-section geometry of the bridge: drawing not to scale.

longitudinal thermal expansion, labeled "exp" in Figure 1, as well as a connection that prevented longitudinal translation, labeled "pinned" in Figure 1, were located at the base of each plate girder, where the girder was supported by a concrete pier or abutment. All subsequent discussions of the bridge will refer to the bridge that carried eastbound traffic, particularly the three eastern spans, which were the only ones tested. A detailed description of the test structure, the experimental procedures described below and all results obtained can be found in reference [38].

4. AMBIENT VIBRATION TEST PROCEDURE

Integral-circuit piezoelectric accelerometers were used for the vibration measurements. Twenty-six 2·54 cm square (1 in square) aluminum mounting blocks were dental cemented to the inside web of the plate girder at mid-height and at the axial locations shown in Figure 3. Within a span the three blocks were equally spaced in the axial direction. Accelerometers were mounted on the blocks with a 10–32 stud, in the global Y direction shown in Figure 3. These accelerometers had a nominal sensitivity of 1 V/g, a specified frequency range of 1–2000 Hz, and an amplitude range of $\pm 4\,g$. Two-conductor 20 gauge cable ranging from 21·3 m to 88·9 m (70 ft to 291 ft) connected the accelerometers

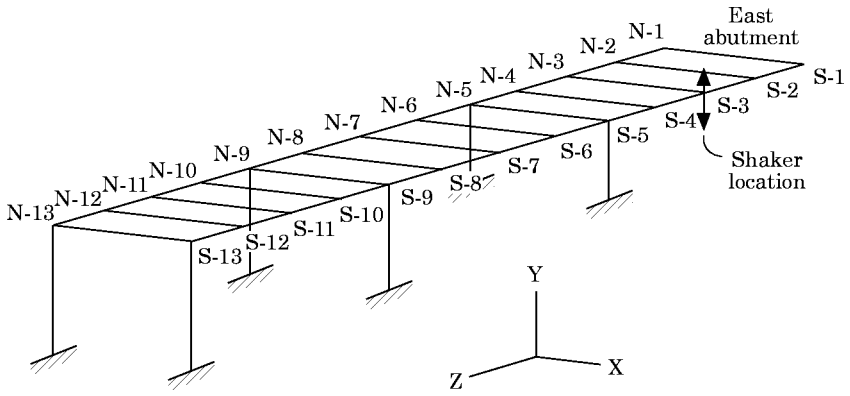

Figure 3. The accelerometer locations.

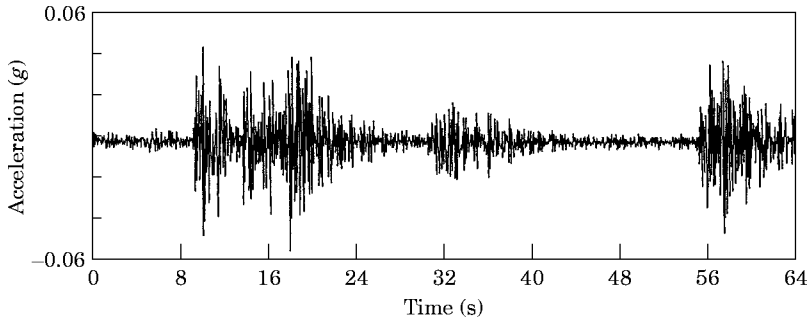

Figure 4. A typical time-history measured at location S-7 during ambient vibration tests.

to the data acquisition system. The data acquisition system used in the modal tests consisted of a computer workstation, which controlled 29 input modules, and a signal processing module. The workstation was also the platform for a commercial data acquisition/signal analysis/modal analysis software package. The input modules provide power to the accelerometers and performed analog to digital conversion of the accelerometer voltage–time histories. The signal processing module performed the needed fast Fourier transform calculations. A 3500 watt AC generator was used to power this system in the field.

During the tests, traffic had been directed on to the two northern lanes. Significantly different traffic flow could be observed at various times when data was being acquired. During morning and afternoon rush hours the traffic would slow down considerably, thus producing lower level excitations in the bridge. At midday the trucks crossing the bridge at high speeds would cause higher level excitations that would often over range some of the data acquisition channels. A final ambient vibration test was conducted just prior to the subsequent forced vibration tests, when all traffic had been removed from the eastbound bridge. For this test the ambient vibration source was provided by the traffic on the adjacent new eastbound bridge and the existing westbound bridge that was transmitted through the ground to the piers and abutment. During all ambient tests, no attempt was made to characterize the input to the bridge. Although the assumption that the traffic on a bridge produces a white noise input was not verified; the random weights of vehicles, as discussed by Turner and Pretlove [39], their random arrival times, the random nature of the vehicles' suspension systems, and the randomly distributed road surface irregularities suggest that this assumption is valid.

TABLE 1

Ambient vibration test summary

Test designation	Frequency range (Hz)	Number of averages	Reference channel*	Time
t1tr	0–6·25	100	S-2	9:27 a.m.–12:17 p.m.
t10tr	0–6·25	35	S-6	2:42–3:30 p.m.
t15tr†	0–12·5	15	S-2	4:45–5:00 p.m.

* See Figure 3.

† This test was performed immediately before forced vibration tests when traffic had been routed to new spans. Ambient excitation was caused by traffic on the adjacent spans.

The data acquisition system that was used did not estimate cross-correlation functions directly. Instead, CPS were determined from measured acceleration response data and these functions were inverse Fourier transformed to obtain the needed cross-correlation functions. The CPS were calculated with an additional accelerometer located at either S-2 or S-6 in Figure 3, specified as the reference channel. Sampling parameters were specified that calculated the CPS from 64 s or 32 s time windows discretized with 1024 samples. A typical time history measured at location S-7 is shown in Figure 4. On the basis of these sampling parameters, the CPS were calculated for frequency ranges of 0–6·25 Hz or 0–12·5 Hz. Multiple averages were used to minimize random errors when calculating the CPS. Frequency resolutions, Δf, of 0·015625 Hz and 0·03125 Hz were obtained for the 0–6·25 Hz CPS and 0–12·5 Hz CPS, respectively. A Hanning window was applied to the time signals to minimize leakage and AC coupling was specified to minimize DC offsets. A test of the AC coupling filter showed that the filter did not attenuate the signal at frequencies above 2 Hz, and it was concluded that the AC coupling filter would not adversely affect the data in the frequency ranges of interest. A dynamic range of 3·98 V was specified and time samples that overloaded this range were rejected. With these sampling parameters and the overload reject specified, data acquisition occurred over time periods ranging up to almost three hours. The different ambient vibration tests that were conducted are summarized in Table 1.

5. FORCED VIBRATION TEST PROCEDURE

When traffic was removed from the bridge and the final ambient tests had been complete, forced vibration tests were performed. Eastbound traffic had been transferred to a new

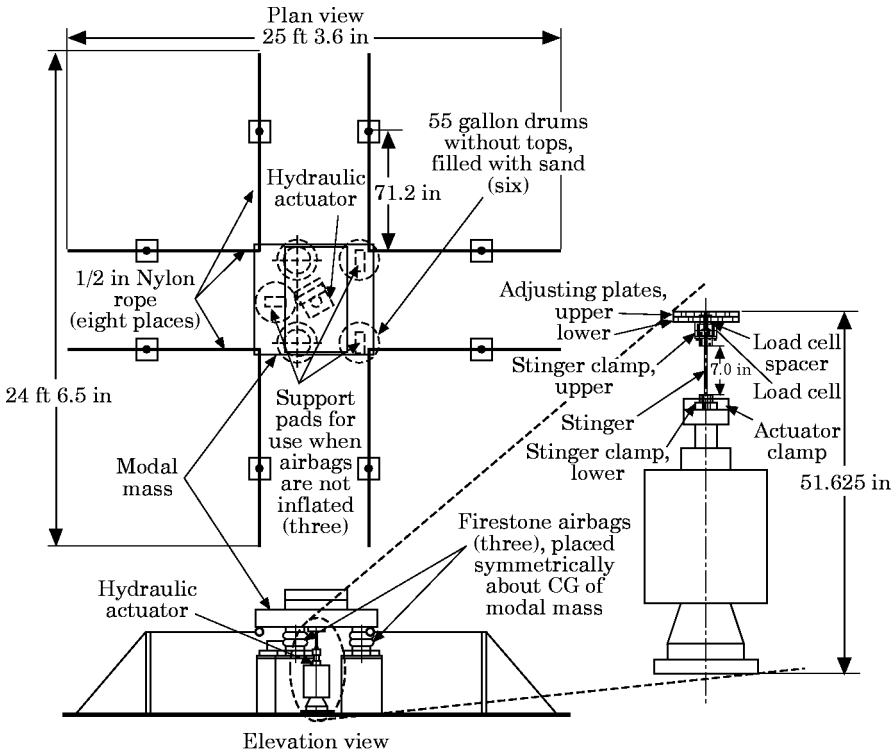

Figure 5. The shaker used in forced vibration tests: 1 ft = 0·3048 m; 1 in = 2·54 cm.

bridge just south of the one being tested. The westbound traffic continued on the original westbound bridge. These forced vibration tests were conducted so that results from a conventional experimental modal analysis of the bridge could be compared with the ambient vibration test results. In this context, experimental modal analysis refers to the procedure whereby a measured force excitation is applied to a structure and the structure's acceleration response is measured at discrete locations that are representative of the structure's motion. Both the excitation and the response time histories are transformed into the frequency domain so that modal parameters (resonant frequencies, mode shapes and modal damping) can be determined by curve fitting a Laplace domain representation of the FRF to the measured frequency domain data [1]. The data acquisition system, mounting blocks, cabling, accelerometers and generator used for the forced vibration tests were identical to those used for the ambient vibration tests. An additional input module was used to monitor the force input.

A hydraulic shaker, shown in Figure 5, was used to generate a measured force input. The shaker consisted of a 96·5 kN (21 700 lb) reaction mass supported by three air springs resting on top of drums filled with sand. A 9·79 kN (2200 lb) hydraulic actuator bolted under the center of the mass and anchored to the top of the bridge deck provided the input force to the bridge. The amplifier gain was controlled to provide an approximately 8·90 kN (2000 lb) peak random force input over a frequency range of 2–12 Hz. An accelerometer mounted on the reaction mass was used to measure the force input to the bridge. This indirect force measurement gives the total force transferred to the bridge through the drums as well as the actuator. The shaker was located over the south plate girder directly above point S-3 as shown in Figure 3. A detailed description of the shaker can be found in reference [40].

Sampling parameters were specified so that responses with frequency content in the range of 0–12·5 Hz could be measured. All computed frequency response functions were based on 30 averages with no overlap. A Hanning window was applied to all time samples used in these calculations. A typical 32 s response time history measured at location S-7 is shown in Figure 6 for comparison with the time history measured during the ambient vibration tests; Figure 4.

6. RESULTS

A typical cross-power spectrum between two response measurements (reference location S-2 and response location N-7) measured during the ambient vibration test designated t1tr

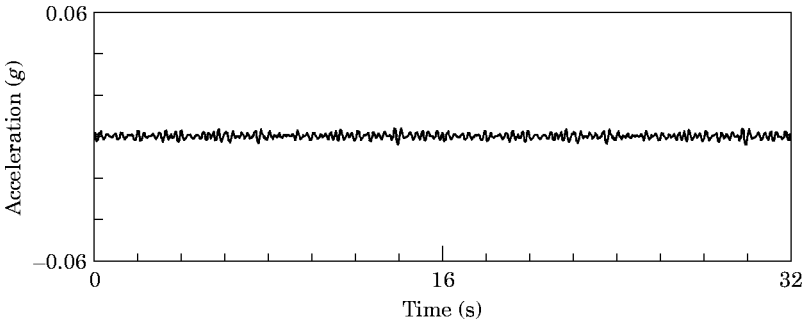

Figure 6. A typical time-history measured at location S-7 during forced vibration tests.

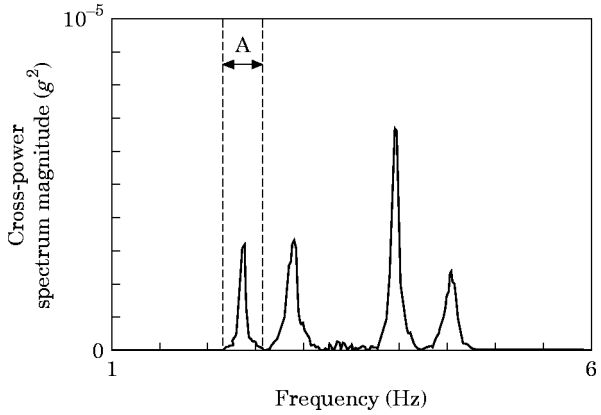

Figure 7. The cross-power spectrum between ambient vibration measurements made at locations S-2 and N-7. The portion of the spectrum between the dashed lines labelled A was analyzed to determine the dynamic properties associated with the first mode.

is shown in Figure 7. The inverse Fourier transform of this measurement yields the cross-correlation function, shown in Figure 8. In practice, a particular peak in the cross-power spectrum was isolated, as shown in Figure 7, by zero-padding the spectrum on either side of the peak. The inverse transform of this modified spectrum yields the cross-correlation function, shown in Figure 9, which was curve-fitted to obtain the resonant frequencies and modal damping values. Each peak in the cross-power spectrum was analyzed in this manner. In Figures 8 and 9 is shown the circular nature of the cross-correlation function as discussed in reference [4]. In practice, only the decaying half of the function shown in Figure 9 was curve-fitted. When closely spaced modes are present,

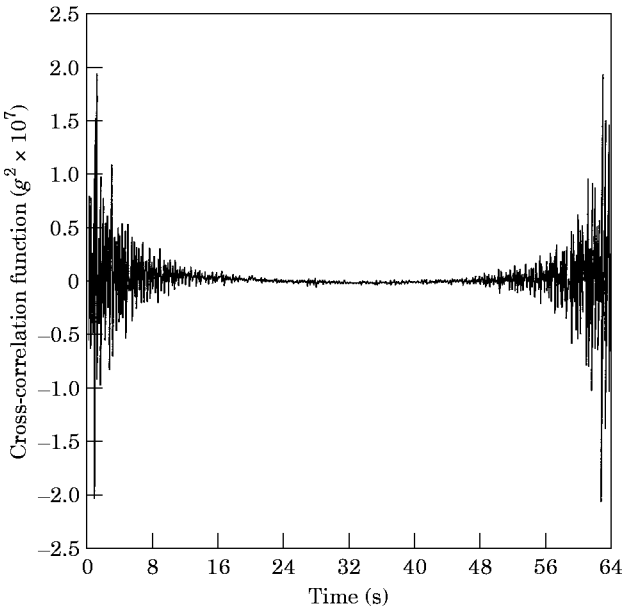

Figure 8. The cross-correlation function obtained from the inverse Fourier transform of the CPS shown in Figure 7.

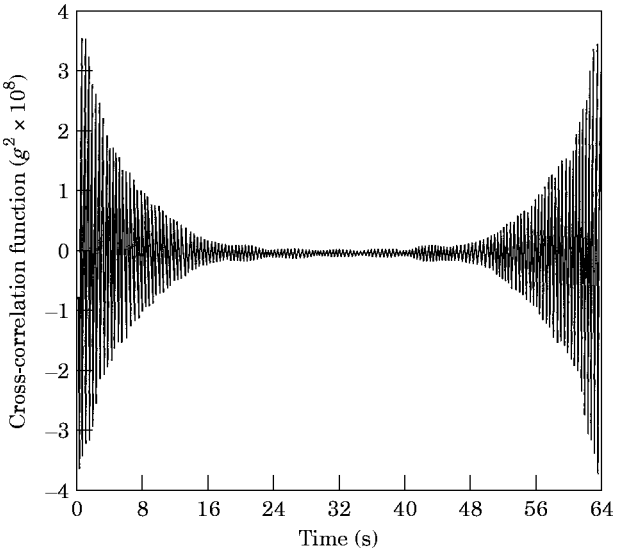

Figure 9. The cross-correlation function corresponding to the isolated portion of the spectrum shown in Figure 7.

the curve-fitting procedure attempts to fit multiple modes to the portion of the spectrum being analyzed. The cross-correlation functions are based on averaged spectra generated from windowed time-histories. The resonant frequencies and modal damping values determined when the ambient vibration parameter identification method was applied to the cross-correlation functions are summarized in Table 2. Both parameters were calculated in a global manner using a complex exponential curve-fitting method; that is, each measured CPS was inversely transformed and the resulting cross-correlation functions were used to estimate the modal parameters. The mean value of these parameters, obtained from individual analysis of the 26 measurements, was then calculated. These mean values appear in Table 2. A detailed discussion of the curve-fitting procedure is given in reference [38]. Also shown in Table 2 are the resonant frequencies and modal damping values determined by conventional modal analysis using a measured input. A rational-fraction polynomial global curve-fitting algorithm in a commercial modal analysis software package [41] was used to fit the analytical models to the measured FRF data and extract resonant frequencies, mode shapes and modal damping values. The magnitude of a typical measured FRF that was analyzed, corresponding to the measurement made at location N-7 in Figure 3, is shown in Figure 10.

The mode shapes for the first six modes, identified from amplitude and phase information contained in the CPS measured during the ambient vibration test designated t1tr, are shown in Figure 11. The corresponding modes identified from the conventional measured input modal analysis are shown in Figure 12. A modal assurance criterion (MAC), sometimes referred to as a modal correlation coefficient [1], was calculated to quantify the correlation between mode shapes measured during different tests. The MAC makes use of the orthogonality properties of the mode shapes to compare modes from different tests. If the modes are identical, a scalar value of one is calculated by the MAC.

TABLE 2

Resonant frequencies and modal damping values identified from ambient vibration response compared with similar properties identified from conventional forced vibration tests

Test	Mode 1, frequency (Hz)/ damping (%)	Mode 2, frequency (Hz)/ damping (%)	Mode 3, frequency (Hz)/ damping (%)	Mode 4, frequency (Hz)/ damping (%)	Mode 5, frequency (Hz)/ damping (%)	Mode 6, frequency (Hz)/ damping (%)
t1tr	2·39/ 1·28	2·92/ 1·18	3·42/ 1·00	3·96/ 0·94	4·10/ 1.58	4·56/ 1.56
t10tr	2·42/ 1·15	2·93/ 1·18	3·46/ 0·85	3·99/ 0·70	4·12/ 0·59	4·61/ 0·97
t15tr	2·52/ 1·28	3·04/ 0·38	3·53/ 0·89	4·10/ 1·08	4·17/ 0·92	4·71/ 0·60
Forced vibration test	2·48/ 1·06	2·96/ 1·29	3·50/ 1·52	4·08/ 1·10	4·17/ 0·86	4·63/ 0·92

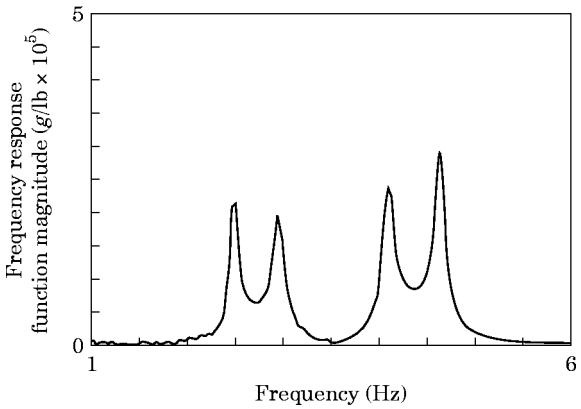

Figure 10. The magnitude of the frequency response function measured at location N-7 during the forced vibration test.

If the modes are orthogonal or otherwise dissimilar, a value of zero is calculated. The MAC that compares modes r and s has the form

$$\mathrm{MAC}\,(r,s) = \frac{\left|\sum_{L=1}^{p} (\phi_L^r)(\phi_L^s)^*\right|^2}{\left(\sum_{L=1}^{p} (\phi_L^r)(\phi_L^r)^*\right)\left(\sum_{L=1}^{p} (\phi_L^s)(\phi_L^s)^*\right)}, \tag{13}$$

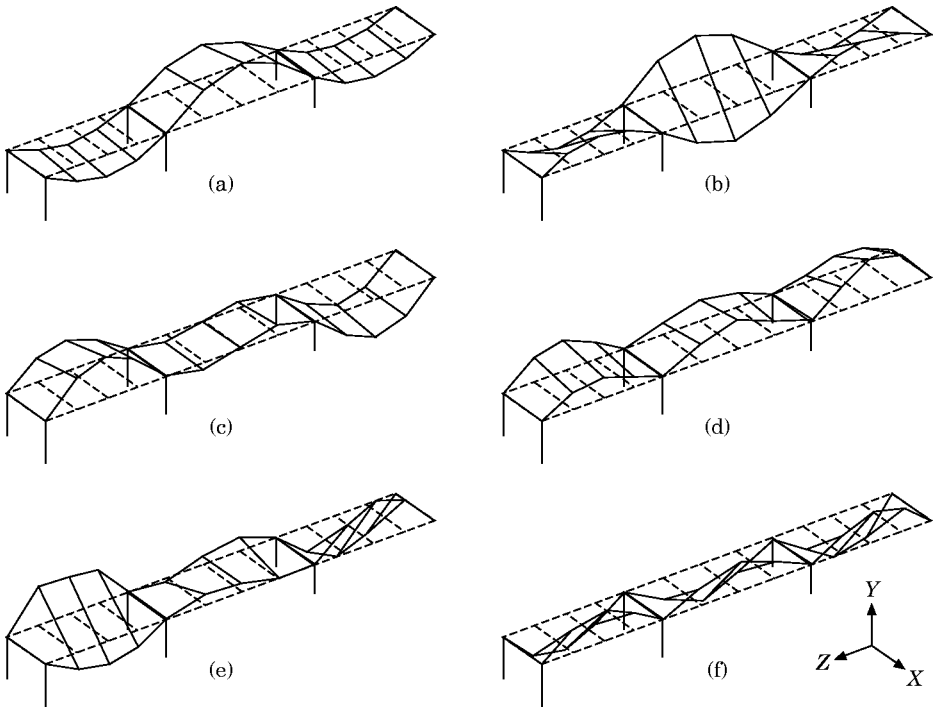

Figure 11. The first six modes identified during ambient vibration tests from relative amplitude and phase information contained in the CPS. (a)–(f) correspond to modes 1–6, respectively.

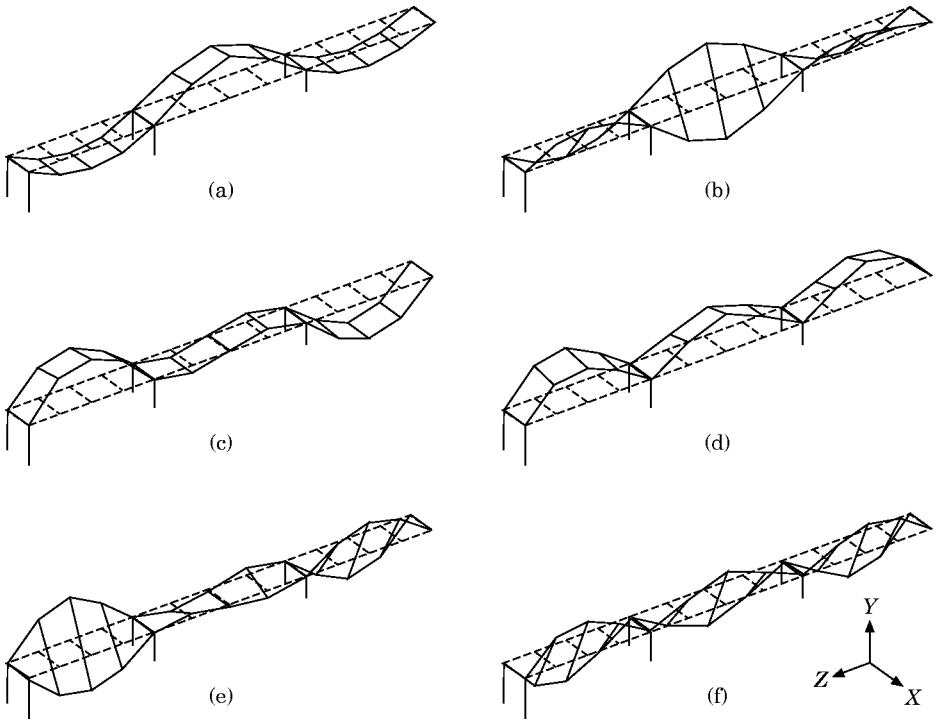

Figure 12. The first six modes identified during the conventional measured forced input vibration test. (a)–(f) correspond to modes 1–6, respectively.

where (ϕ_L^r) and (ϕ_L^s) are elements of p-dimension mode shape vectors, and the asterisk denotes the complex conjugate. Ewins [1] points out that, in practice, correlated modes will yield a value greater than 0·9 and uncorrelated modes will yield a value less than 0·05.

The matrix in Table 3 shows the MACs that compared modes identified from data measured during the ambient test designated t1tr with modes identified during the forced vibration test. This matrix shows that the six modes identified from the ambient vibration data are, in fact, closely correlated with the modes measured during the forced vibration test. A similar correlation was obtained for modes identified from the other ambient vibration tests and modes identified during the forced vibration test. Modes 4 and 5, which are closely spaced in frequency and which were difficult to identify during several ambient vibration tests, did not always show good correlation with the modes determined during the forced vibration tests.

TABLE 3

Modal assurance criteria: *mode shapes identified from ambient vibration test t*1*tr compared with mode shapes identified from forced vibration test*

Mode/test	1/Forced	2/Forced	3/Forced	4/Forced	5/Forced	6/Forced
1/t1tr	0·989	0·008	0·000	0·004	0·002	0·001
2/t1tr	0·004	0·985	0·000	0·001	0·001	0·004
3/t1tr	0·002	0·003	0·984	0·000	0·009	0·001
4/t1tr	0·005	0·002	0·001	0·901	0·102	0·009
5/t1tr	0·000	0·001	0·005	0·066	0·917	0·005
6/t1tr	0·001	0·003	0·002	0·004	0·004	0·984

7. SUMMARY AND CONCLUSIONS

In this study, the cross-correlation function between two response measurements made on an ambiently excited structure was shown to have the form of decaying sinusoids, similar to the system's impulse response function. The significance of this derivation is that standard time domain curve-fitting procedures such as the complex exponential method, which are typically applied to impulse response functions, can now be applied to the cross-correlation functions to estimate the resonant frequencies and modal damping of the structure. The advantage of this system identification method over standard procedures that identify resonant frequencies from peaks in the power spectrum and damping from the width of the power spectrum is the ability to identify closely spaced modes and their associated damping. Also, implementation of this method can be accomplished with algorithms that are typically available in most commercial signal analysis and experimental modal analysis software packages. However, these software packages typically estimate the cross-power spectrum and then inverse Fourier transform this function to obtain the cross-correlation function. Therefore, this method will be subject to window-dependent resolution bias errors, as discussed in reference [37]. The effects of such error sources were not investigated in this study. Random errors were minimized by averaging numerous measurements when estimating the cross-power spectra.

The derivation presented in this paper, which shows that the impulse response function and the cross-correlation function are of similar form, was based on the assumption that the ambient vibration source is a white noise random process. Although the assumption that the traffic on a bridge produces a white noise input was not verified; the random weights of vehicles, as discussed by Turner and Pretlove [39], their random arrival times, the random nature of the vehicles' suspension systems, and the randomly distributed road surface irregularities suggest that this assumption is valid.

The ambient vibration system identification method was applied to an in-service highway bridge where traffic provided the vibration source. Subsequently, after traffic had been re-routed, the same bridge was tested with conventional measured-input force vibration procedures. The results from these tests allow the following conclusions to be made:

1. Ambient vibration from traffic provides an adequate source of input for identifying the dynamic properties of the bridge. The results obtained with the method developed in this study were repeatable (resonant frequency values measured with traffic on the bridge did not vary by more than 2%) and were independent of the selected reference measurement.

2. The method presented in this paper was able to discern closely spaced modes (0·07 Hz or approximately 2·24 Δf apart) such as modes 4 and 5, and this method identified the associated modal damping values for these modes. These modes showed coupling through the off-diagonal MAC values. However, both the ambient system identification method and the conventional measured-input system identification method were able to identify the dynamic properties associated with these modes.

3. All measured modes were lightly damped, with modal damping values ranging from 0·38% to 1·58%. These modes can be accurately approximated as real modes. The phase angles of the CPS associated with the resonant frequency were typically close to either 0 or 180 degrees. An average modal damping value of 1·01% was obtained from the three ambient tests. The forced vibration test yielded an average modal damping value of 1·12%, a 9·82% difference from the ambient results. The identified values are consistent with those obtained by other investigators for similar bridges as summarized in references [28, 31, 42].

4. During test t15tr, when traffic was not on the bridge, and during the forced vibration test, slightly higher frequencies were measured for each mode as compared to the results

from tests when traffic was on the bridge. These higher frequencies are attributed to the reduced mass of the system that resulted when traffic was removed from the bridge. Within the limits of the traffic flows that were monitored, a comparison of the results from tests when traffic on the bridge was used as the excitation source (tests t1tr and t10tr) and results from test t15tr quantifies the variations in the dynamic properties that can result from varying traffic loads. Resonant frequencies for the first six modes were found to be from 1·44% to 4·37% higher when there was no traffic on the bridge. The average modal damping value was 0·86% without traffic, as compared to 1·08% when traffic was present. Although not quantified, visual inspection of the animated mode shapes revealed that they were not affected by the removal of traffic.

5. Background sources of ambient vibration from traffic on the adjacent bridges were of sufficient magnitude that the dynamic properties of the structure could be determined by measuring the response to this excitation source as was done in test t15tr.

This experimental verification of the accuracy of the ambient vibration system identification method implies that the proposed method can be used accurately to assess the dynamic properties of bridges and other structures in a non-intrusive manner. Currently, there are numerous studies under way to develop methods for monitoring the structural integrity of bridges by examining changes in their dynamic properties [43]. One goal of this research is to develop remotely monitored, *in situ* damage assessment systems for the bridge. If damage identification procedures that examine changes in dynamic properties are to become part of an *in situ*, remote monitoring system, then from a practical viewpoint they will have to work with dynamic properties identified from ambient excitation of the bridge. The ambient system identification method reported in this study is amenable to such an *in situ* monitoring system.

ACKNOWLEDGMENTS

Funding for this research was provided by the Federal Highway Administration through a project administered and jointly performed by New Mexico State University. The authors would like to acknowledge the co-operation and teamwork that was exhibited by all parties involved in these tests, including faculty, technicians and students from New Mexico State University, numerous people at the New Mexico State Highway and Transportation Department, and the staff at the Alliance for Transportation Research.

REFERENCES

1. D. J. Ewins 1985 *Modal Testing*: *Theory and Practice*. New York: John Wiley.
2. V. R. McLamore, G. C. Hart and I. R. Stubbs 1971 *Proceedings of the American Society of Civil Engineers*, *Journal of the Structural Division* **97**, 2567–2582. Ambient vibration of two suspension bridges.
3. R. Crawford and H. S. Ward 1964 *Bulletin of the Seismological Society of America* **54**, 1743–1756. Determination of the natural periods of buildings.
4. J. S. Bendat and A. G. Piersol 1980 *Engineering Applications of Correlation and Spectral Analysis*. New York: John Wiley.
5. A. M. Abdel-Ghaffar and G. W. Housner 1978 *Journal of the Engineering Mechanics Division* **104**, 983–999. Ambient vibration tests of suspension bridge.
6. P. G. Buckland, R. Hooley, B. D. Morgenstern, J. H. Rainer and A. M. van Selst 1979 *Journal of the Structural Division* **105**, 859–874. Suspension bridge vibrations: computed and measured.
7. R. Shepherd, H. E. E. Brown and J. H. Wood 1979 *Proceedings of the Institution of Civil Engineers*, *Part* 1 **66**, 457–469. Dynamic investigations of the Mohaka river bridge.
8. B. M. Douglas, C. D. Brown and M. L. Gordon 1981 *Conference on Dynamic Response of*

Structures: *Experimentation*, *Observation*, *Prediction and Control*, 98–712. Experimental dynamics of highway bridges.

9. G. C. Pardoen, A. J. Carr and P. J. Moss 1981 *Proceedings of the Second Specialty Conference on Dynamic Response of Structures*: *Experimentation*, *Observation*, *Prediction and Control*, 29–45. Bridge modal identification problems.
10. J. H. Gates and M. J. Smith 1982 *FHWA/CA/SD*-82/07. Verification of dynamic modeling methods by prototype experiments.
11. J. W. G. Van Nunen and A. J. Persoon 1982 *Engineering Structures* **4**, 99–105. Investigation of the vibrational behavior of a cable-stayed bridge under wind loads.
12. H. Tanaka and A. G. Davenport 1983 *Journal of Engineering Mechanics* **109**, 296–312. Wind-induced response of Golden Gate bridge.
13. A. M. Abdel-Ghaffar and R. H. Scanlan 1985 *Journal of Engineering Mechanics* **111**, 463–482. Ambient vibration studies of Golden Gate bridge, I: suspended structure.
14. A. M. Abdel-Ghaffar and R. H. Scanlan 1985 *Journal of Engineering Mechanics* **111**, 483–499. Ambient vibration studies of Golden Gate bridge, II: pier–tower structure.
15. J. M. White and G. C. Pardoen 1987 *Proceedings of the* 5*th International Modal Analysis Conference* **1**, 16–20. Modal identification of the Golden Gate bridge tower using ambient vibration data.
16. H. S. Ward 1984 *Journal of Structural Engineering* **110**, 2487–2498. Traffic generated vibrations and bridge integrity.
17. L. A. Taskov 1988 *Conference on Earthquake and Civil Engineering Dynamics*, 81–92. Dynamic testing of bridge structures applying force and ambient vibration methods.
18. J. M. Brownjohn, A. A. Dumanoglu, R. T. Severn and C. A. Taylor 1987 *Proceedings of the Institute for Civil Engineering*, *Part* 2 **83**, 561–600. Ambient vibration measurements of the Humber suspension bridge and comparison with calculated results.
19. J. M. Brownjohn, A. A. Dumanoglu, R. T. Severn and A. Blakeborough 1989 *Earthquake Engineering and Structural Dynamics* **18**, 263–283. Ambient vibration survey of the Bosporus suspension bridge.
20. T. Kumarasena, R. H. Scanlon and G. R. Morris 1989 *Journals of Structural Engineering* **115**, 2313–2328. Deer Isle bridge: field and computed vibrations.
21. J. C. Wilson and T. Liu 1991 *Earthquake Engineering and Structural Dynamics* **20**, 723–747. Ambient vibration measurements on a cable-stayed bridge.
22. D. Muria-Vila, R. Gomez and C. King 1991 *Journal of Structural Engineering* **117**, 3396–3416. Dynamic structural properties of cable-stayed Tampico bridge.
23. J. M. Brownjohn, A. A. Dumanoglu and R. T. Severn 1992 *Earthquake Engineering and Structural Dynamics* **21**, 907–924. Ambient vibration survey of the Faith Sultan Mehmet (second Bosporus) suspension bridge.
24. P. Paultre, J. Proulx and M. Talbot 1995 *Journal of Structural Engineering* **121**(2), 362–376. Dynamic testing procedures for highway bridges using traffic loads.
25. C. A. M. de Smet, A. J. Felber, R. Cantieni and C. Kramer 1996 *Proceedings of the* 14*th International Modal Analysis Conference* **1**, 63–69. Ambient vibration study of the new Rhein bridge for highway N4.
26. A. Felber, R. Cantieni and C. A. M. de Smet 1996 *Proceedings of the* 14*th International Modal Analysis Conference* **1** 233–239. Ambient vibration study of the Ganter bridge.
27. A. J. Felber and C. E. Ventura 1996 *Proceedings of the* 14*th International Modal Analysis Conference* **1,** 459–465. Frequency domain analysis of the ambient vibration data of the new Queensborough bridge main span.
28. E. Giorcelli, L. Garibaldi, A. Riva and A. Fasana 1996 *Proceedings of the* 14*th International Modal Analysis Conference* **1**, 466–469. ARMAV analysis of Queensborough bridge ambient data.
29. J. C. Asmussen, S. R. Ibrahim and R. Brinker 1996 *Proceedings of the* 14*th International Modal Analysis Conference* **1**, 453–458. Random decrement and regression analysis of traffic response of bridges.
30. A. De Stefano, M. Knaflitz, P. Bonato, R. Ceravolo and G. Gagliati 1996 *Proceedings of the* 14*th International Modal Analysis Conference* **1**, 470–476. Analysis of ambient vibration data from Queensborough bridge using Cohen class time–frequency distributions.
31. R. Brinker, A. De Stefano and B. Piombo 1996 *Proceedings of the* 14*th International Modal Analysis Conference* **1**, 477–482. Ambient data to analyse the dynamic behaviour of bridges: a first comparison between different techniques.
32. G. H. James, T. G. Carne and J. P. Lauffer 1993 *Sandia National Laboratory*, *Report SAND*,

92–1666. The natural excitation technique (NExT) for modal parameter extraction from operating wind turbines.
33. G. H. James, T. G. Carne and J. P. Lauffer 1995 *Modal Analysis* **10**, 260–277. The natural excitation technique (NExT) for modal parameter extraction from operating structures.
34. H. Vold and G. F. Rocklin 1982 *Proceedings of the* 1*st International Modal Analysis Conference*, 542–548. The numerical implementation of a multi-input modal estimation method for mini-computers.
35. D. L. Brown, R. J. Allemang, R. Zimmerman and M. Mergeay 1979 *Society of Automotive Engineers*, *Technical Paper* 790221. Parameter estimation techniques for modal analysis.
36. J. N. Juang and R. S. Pappa 1985 *Journal of Guidance*, *Control*, *and Dynamics* **8**, 620–627. An eigensystem realization algorithm for modal parameter identification and model reduction.
37. H. Schmidt 1985 *Journal of Sound and Vibration* **101**, 377–404. Resolution bias errors in spectral density, frequency response, and coherence function measurements, III: application to second-order systems (white noise excitation).
38. C. R. Farrar, W. E. Baker, T. M. Bell, K. M. Cone, T. W. Darling, T. A. Duffey, A. Eklund and A. Migliori 1994 *Los Alamos National Laboratory*, *Report LA*-12767-*MS*. Dynamic characterization and damage detection in the I-40 bridge over the Rio Grande.
39. J. D. Turner and A. J. Pretlove 1988 *Journal of Sound and Vibration* **122**, 31–42. A study of the spectrum of traffic-induced bridge vibration.
40. R. L. Mayes and M. A. Nusser 1994 *Sandia National Laboratory*, *Report SAND* 94-0228. The Interstate-40 bridge shaker project.
41. Structural Measurements Systems 1987 *Modal* 3·0. San Jose, California.
42. G. P. Tilly 1977 *Transportation and Road Research Laboratory*, *Crowthorne*, *Berkshire*, *U.K.* Damping of highway bridges: a review symposium on dynamic behavior of bridges.
43. S. W. Doebling, C. R. Farrar, M. B. Prime and D. W. Shevitz 1996 *Los Alamos National Laboratory*, *Report LA*-13070-*MS*. Damage identification and health monitoring of structural and mechanical systems from changes in their vibration characteristics: a literature review.